Neurochemistry International 128 (2019) 186–195

Contents lists available at ScienceDirect

Neurochemistry International

journal homepage: www.elsevier.com/locate/neuint

Early neurochemical modifications of monoaminergic systems in the R6/1 mouse model of Huntington's disease

Emilie Puginier[a,1], Rahul Bharatiya[a,b,1], Abdeslam Chagraoui[c], Julien Manem[a], Yoon H. Cho[a], Maurice Garret[a,2], Philippe De Deurwaerdère[a,*,2]

[a] Centre National de La Recherche Scientifique-Unité Mixte de Recherche 5287, 33076, Bordeaux Cedex, France
[b] Department of Biomedical Sciences, Section of Neuroscience and Clinical Pharmacology, University of Cagliari, SS 554, Km 4,500, 09042, Monserrato, Cagliari, Italy
[c] Normandie Univ, UNIROUEN, INSERM, U1239, CHU Rouen, Neuronal and Neuroendocrine Differentiation and Communication Laboratory, Institute for Research and Innovation in Biomedicine of Normandy (IRIB), Department of Medical Biochemistry, Rouen University Hospital, Rouen, France

ARTICLE INFO

Keywords:
Dopamine
DOPAC
Serotonin
5-HIAA
Noradrenaline
HPLC
Correlative analysis
Neurochemistry
Cortex
Striatum
Mesencephalon
Connectivity

ABSTRACT

Huntington's disease (HD) is a rare, autosomal neurodegenerative disease characterized by motor and cognitive impairments appearing in adults. The R6/1 mouse model of the disease recapitulates the adult onset of motor symptoms preceded by cognitive and affective deficits. The monoaminergic systems participate in the establishment of motor and cognitive loops and we postulated that their organization and interaction could be precociously altered. Using tissue measurement of dopamine (DA), serotonin (5-HT), noradrenaline, and some metabolites, we observed that DA and/or its metabolite 3,4-dihydroxyphenylacetic acid (DOPAC), but not 5-HT or noradrenaline tissue content was reduced in an age-dependent manner (from two to six months) in the striatum, substantia nigra and globus pallidus of R6/1 mice. The metabolite of 5-HT was also lower in R6/1 mice, mainly in the substantia nigra and hippocampus. We then addressed early disorganization of monoaminergic systems in 18 brain regions encompassing several neurobiological networks in 35 day-old animals. DA tissue content was not altered in the striatum or substantia nigra but was decreased in the nucleus accumbens and increased in the globus pallidus. The correlations of monoaminergic index in-between the 18 selected brain regions revealed distinct organizations of monoamines in R6/1 mice, notably marked by a loss of the number of correlations of the DOPAC/DA ratio. The neurochemical analyses show that each monoaminergic system is distinctly altered in the R6/1 mouse model. The early abnormal organization of these systems likely points out altered maturation of neurobiological networks at early stages of HD.

1. Introduction

Huntington's disease (HD) is a rare, autosomal, and dominant neurodegenerative disease. The abnormal number of repetitions of the triplet of nucleotides CAG in the gene encoding the protein huntingtin is responsible for the disease. HD is characterized by motor impairments appearing at the age of 35–45 years old which are often preceded or accompanied by cognitive and behavioural symptoms (Martinez-Horta et al., 2016; Ramos and Garrett, 2017). It suggests multiple and progressive alterations in neurobiological networks beyond the canonical cortico-striatal pathways.

The monoaminergic systems, i.e. dopamine (DA), serotonin (5-hydroxytryptamine, 5-HT), and noradrenaline (NA) reach motor and cognitive loops in the brain from the brainstem regions including substantia nigra (SN) and ventral tegmental area (VTA) for DA, the dorsal and median raphe nuclei (DRN and MRN, respectively) for 5-HT, and the locus coeruleus for NA. These neuronal systems establish numerous interactions with neurobiological networks and are thought to participate in the maturation of executive functions (Dalley et al., 2011; De Deurwaerdere and Di Giovanni, 2017; Dellu-Hagedorn et al., 2018; Pittaras et al., 2016; Simic et al., 2017). The data in humans carrying the HD mutation reveal a reduction of the nigrostriatal DA neuronal function although this has been a matter of debate for several years (Bedard et al., 2011; Cepeda et al., 2014; Chen et al., 2013). The activity of 5-HT neurons would be upregulated at least in the striatum (Bedard et al., 2011; Kish et al., 1987). In transgenic rodent models,

* Corresponding author. Institut des Neurosciences Cognitives et Intégratives d'Aquitaine, UMR CNRS 5287, 146, Rue Léo Saignat, 33076, Bordeaux, France.
E-mail address: deurwaer@u-bordeaux.fr (P. De Deurwaerdère).
[1] The authors have equally participated.
[2] The authors have equally participated.

https://doi.org/10.1016/j.neuint.2019.05.001
Received 26 February 2019; Received in revised form 13 April 2019; Accepted 1 May 2019
Available online 02 May 2019
0197-0186/

Abbreviations

Am	(amygdala)
aMC	(motor cortex M2, anterior part)
Cb	(cerebellum)
DA	(dopamine)
DLS	(dorsolateral striatum)
DMS	(dorsomedial striatum)
DOPAC	(3,4-dihydroxyphenylacetic acid)
DRN	(dorsal raphe nucleus)
dHP	(dorsal part of the hippocampus)
GP	(globus pallidus pars externa)
HPLC	(high pressure liquid chromatography)
HVA	(homovanillic acid)
IL	(infralimbic cortex)
NA	(noradrenaline)
nAC	(nucleus accumbens)
OFC	(orbitofrontal cortex)
PL	(prelimbic cortex)
pMC	(motor cortex M2 and cingulate cortex, posterior part)
PND35	(postnatal day 35)
5-HIAA	(5-hydroxyindole-3-acetic acid)
5-HT	(5-hydroxytryptamine; serotonin)
SN	(substantia nigra)
Th	(thalamus)
vHP	(ventral part of the hippocampus)
VLS	(ventrolateral striatum)
VMS	(ventromedial striatum)
VTA	(ventral tegmental area)

most (Garcia-Miralles et al., 2016; Hickey et al., 2002; Johnson et al., 2007; Kaplan et al., 2018; Ortiz et al., 2010, 2011; Reynolds et al., 1999) but not all data (Jahanshahi et al., 2010; Pineda et al., 2005) report a decrease in DA content in the striatum and other brain regions. 5-HT and/or NA tissue contents would also be diminished in the YAC128 and/or R6/2 mice at motor symptomatic stages (Garcia-Miralles et al., 2016; Reynolds et al., 1999). The alterations of DA, 5-HT and/or NA systems could occur before the onset of motor symptoms in R6/1 and R6/2 mice (Mochel et al., 2011; Renoir et al., 2011, 2014bib_Renoir_et_al_2014bib_Renoir_et_al_2011; Reynolds et al., 1999) with distinct temporality of alterations between the few regions investigated.

The motor symptoms in the R6/1 mouse model of HD develop more progressively compared to its cognate model R6/2 mice (Menalled and Chesselet, 2002) and are preceded by numerous behavioural and cognitive abnormalities (Cabanas et al., 2017; Du et al., 2016; Renoir et al., 2011, 2014). This suggests that corresponding neurobiological networks are precociously altered. Tissue levels of monoamines interact with the networks which can be indirectly assessed through the study of multiple correlations of tissue levels across brain regions (Dellu-Hagedorn et al., 2017; Fitoussi et al., 2013; Klouche et al., 2015). We postulated that the brain pattern of monoamines could be early altered in the development of the disease in R6/1 mice.

In the present study, we have analysed at early stage the tissue levels of DA, NA, 5-HT, and some metabolites in multiple parts of the brain of R6/1 and wild-type (WT) mice to perform a qualitative approach addressing brain monoamines connectivity. The age of mice [post-natal day 35 (PND35)] was chosen to have minimal or no quantitative changes of monoamines which would be confounding factors for the correlative analysis. Due to some controversial data on monoamine alteration in R6/1 mice (Petersen et al., 2002; Pineda et al., 2005; Renoir et al., 2014), the age of 35 days was determined after a pilot experiment performed in 2, 4, and 6 month-old mice.

2. Experimental procedures

2.1. Animals

Experiments were performed on male R6/1 transgenic littermate and wild-type (WT) mice of different ages. In a first series of experiments, mice of 2, 4 and 6 months were considered (n = 4–5 animals/group at each age) because they represent pre-symptomatic, early motor symptomatic and late symptomatic motor stages, respectively (Cabanas et al., 2017). In a second series of experiments, only mice of 5 weeks (PND35, n = 11 mice/genotype) were used based on the results of the first experiment. The animals were obtained from a parent genitor R6/1 mouse (B6.Cg-Tg(HDexon1)61Gpb/J, Stock number: 006471, Jackson Laboratory, Main Harbor, NY, USA) crossed with female C57BL/6 mice (IFFA/Credo, Lyon, France). The breeding was done in one animal facility of the University of Bordeaux where WT and R6/1 littermates were group-housed. The R6/1 line expresses exon 1 of the human HD gene with an expanded number of CAG trinucleotide repeats (123.64 ± 0.89). Genotypes were tested by PCR of tail biopsy specimens (Cabanas et al., 2017).

Animals were housed in polycarbonate standard cages (33 × 15 × 14 cm in size; Tecniplast, Limonest, France). The animals were maintained in a colony room under temperature (22 °C) and humidity-controlled (55%) conditions with a 12:12 h light–dark cycle (lights on at 7 am). All animals used procedures conformed to European Economic Community (86–6091 EEC) and the French National Committee guidelines (*décret* 87/848, Ministère de l'Agriculture et de la Forêt) for the care and use of laboratory animals and were approved by the Ethical Committee of Centre National de la Recherche Scientifique, Région Aquitaine-Limousin.

2.2. Tissue processing for histological verification and post-mortem analysis

Before the sacrifice, the mice were gently taken outside the vivarium to be immediately anesthetized with isoflurane during 10 s. The time of sacrifice was between 10:00 a.m. and 12:00 p.m. They were sacrificed by cervical translocation and decapitated (within a few seconds) in a quiet room next door. Brains were rapidly removed, and immersed in isopentane maintained at −35 °C during 2 min. They were stored until dissection at −80 °C. Dissection of brain areas was performed in a cryostat maintained at −26 °C (Chagraoui et al., 2019) with the help of a mouse brain atlas (Franklin and Paxinos, 2007). Bilateral punches of discrete regions were selected using a magnifying glass from brain and collected with cut pipetting tips or stainless steel cannulae of 500 or 800 μm inner diameters. Bilateral punches of one brain region of single mice were pooled. They were collected by an experimenter blind of the genotype. In the first experiment (mice of 2, 4 and 6 months), the punches were taken from the whole striatum, the substantia nigra (SN), the motor cortex, the dorsal and ventral hippocampus (dHP and vHP), the thalamus and the globus pallidus (GP). In second experiment, punches were taken from 18 brain regions. At variance with the other brain regions, the cerebellum (Cb) was grossly taken when it was dissociated from the brain. Fig. 1 depicts the various areas sampled in the present study for the second experiment (without reporting the Cb). The main differences with the first experiment were for the striatum for which a large piece of tissue was taken irrespective of the different quadrants, and for the cortex with no attempt to precisely focus on specific parts. As previously indicated (Fitoussi et al., 2013), a camera was used to picture the location of all punched brain regions.

Samples were transferred in small, labelled tubes (0.6 ml volume) that were pre-weighed on a precision balance, and stored at −80 °C. On the day of the biochemical analysis, the tubes containing the pieces of

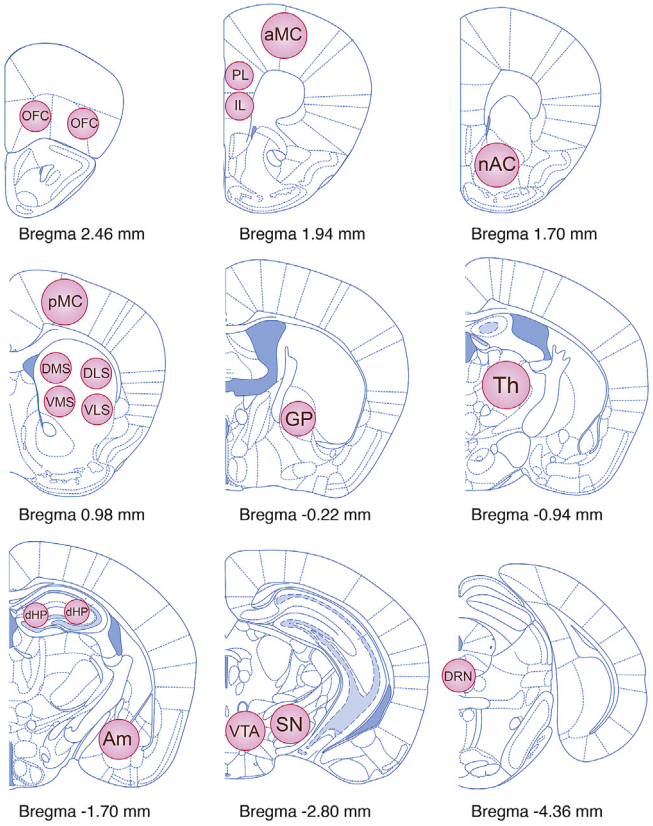

Fig. 1. The illustrations report the approximate position of punched brain regions from coronal sections of WT and R6/1 mice brain (adapted from (Franklin and Paxinos, 2007). The punched tissues were taken in a cryostat from 6 brain regions in the first experiment and 18 regions in the second experiment. Abbreviations are reported in Table 2.

tissue were placed on ice, and were quickly wiped and weighed on the same balance (Dellu-Hagedorn et al., 2017). Tissues were homogenized in 50 or 100 µl of 0.1N $HClO_4$ depending on the weight, sonicated, and centrifuged at 13,000 rpm for 30 min at 4 °C. Aliquots (10 or 20 µl) of the supernatants were injected once in full-loop mode into the HPLC system.

2.3. Chromatographic analysis

Tissue levels of NA, DA, 5-HT and their metabolites were measured by a HPLC-ECD system. Samples (placed on ice after the centrifugation) were injected using a manual injector (Rheodyne 7725i, C.I.L.-Cluzeau, Sainte-Foy-La-Grande, France) equipped with a 10 or 20 µl loop into the HPLC column (Hypersyl C18, 150 × 4.6 mm, 5 µm; C.I.L.-Cluzeau) preceded by a Brownlee–Newgard precolumn (RP-8, 15 × 3.2 mm, 7 µm; C.I.L.-Cluzeau). The composition of the mobile phase was as follows (in mM): 60 NaH_2PO_4, 0.1 Disodium EDTA, 2-Octane-sulfonic acid in deionized water (18 MΩ cm^2) containing 7% methanol. The mobile phase was filtered using 0.22 mm Millipore filter. It was delivered at 1.2 mL/min flow rate using a HPLC pump (LC20-AD, Shimadzu, France). The pH was adjusted approximately around 4 with orthophosphoric acid to get a good separation of the eluents in the chromatogram.

Detection of NA, DA and its metabolites 3,4-dihydroxyphenylacetic acid (DOPAC) and homovanillic acid (HVA), 5-HT and its metabolite 5-hydroxyindole-3-acetic acid (5-HIAA) was performed with a coulometric cell (5011 coulometric cell, ESA, Paris, France) coupled to a programmable detector (Coulochem II, ESA). The potentials of the electrodes were set at −270 mV and +350 mV. The electrochemical signals were recorded via an interface (Ulyss) on a computer equipped with the Azur software (Toulouse, France). In the first experiment, less attention was dedicated to the sensitivity especially for DA and its metabolites. Consequently, the electrochemical signal produced by DA and its metabolites were not detected in the hippocampus, thalamus and the cortex. In the second experiment, the changes of gain programmed during the acquisition were precisely set to increase the sensitivity of detection (Chagraoui et al., 2019). Under these second conditions, the sensitivity for NA, DA, DOPAC, HVA, 5-HT and 5-HIAA was 8, 2, 4, 20, 8 and 5 pg/sample, respectively, with a signal/noise ratio of at least 3:1. The time of elution for a sample was 20–30 min. Calibration curves were performed using a range of concentrations of eluents compatible with the expected quantities (ng range for DA in the striatum; pg range for the hippocampus). Standard solutions containing all the compounds of interest at known concentrations were systematically injected each day before and after a series of samples.

2.4. Data analysis

The tissue levels of monoamines and metabolites were expressed in pg/mg of tissue weight. The index of the turnover corresponding to the ratio between the metabolite and the neurotransmitter (DOPAC/DA and 5-HIAA/5-HT) was also calculated. For each brain region and age, the data are presented as the mean ± SEM of values. Aberrant data were discarded on the basis of the value outside the range of the average mean ± two standard deviations (Fitoussi et al., 2013). The loss of values concerned an aberrant determination of the weight of the tissue, a loss of electrochemical signal (HVA at 6 months in the SN for instance, Table 1), accidental manipulations, a low sensitivity (HVA in the dHP, Table 3a), contaminations of chromatograms (NA in the aMC, Table 3b), and unexplained, rare outliers.

The statistical analysis was performed using a Student's t-test comparing the data obtained in WT and R6/1 mice for all eluents or the ratios, at each age. The Student's t-test was chosen over a one-way ANOVA in the first experiment because the constitution of the cohort occurred at different periods, the age being not considered as an independent variable in the experimental design in contrast to the genotype. Correlations, performed using Bravais-Pearson's correlation test, were made on the content of each monoamine for the second experiment. For each kind of multiple comparison analysis (Fitoussi et al., 2013), within and between monoamine systems, p-values were adjusted using the False Discovering Rate (FDR) controlling procedures (Benjamini and Hochberg, 1995). Correlations were then considered as significant at the 5% level.

3. Results

The first series of experiment studied the quantitative distribution of NA, DA and 5-HT neurochemical indexes in several brain regions at 2, 4 and 6 months of age (Table 1). The quantity of tissue DA in the striatum was significantly lower in R6/1 mice at 2, 4 and 6 months, reaching 32, 57 and 82% decrease compared to values in WT. Similarly, DOPAC tissue content was dramatically decreased in an age-dependent manner in R6/1 mice compared to WT. The levels of HVA were also lower with a significant decrease observed at 4 and 6 months age of R6/1 mice. In the SN, the DA and DOPAC tissue contents were significantly lower in R6/1 mice compared to WT with a decrease estimated at 50% at 4 and 6 months, but for HVA the significant decrease in tissue content was observed only at 4 months. A significant decrease in DA tissue content was reported in the GP in R6/1 mice at 4 and 6 months whereas DOPAC tissue contents were more difficult to analyze due to high variability.

Neurochemical indexes of the 5-HT system were modified in R6/1 compared to WT but the modifications were diffuse and did not similarly affect 5-HT and 5-HIAA. At 2 months, 5-HIAA tissue content was significantly lower in the SN and the vHP. It was also decreased in the striatum of R6/1 at 6 months. No significant modification of the 5-HT content was found in R6/1 mice. However, the turnover index 5-HIAA/

Table 1
Quantitative distribution of DA, 5-HT, and NA neurochemical indexes in some brain regions of mice at 2, 4, and 6 months of age.

	2 m		4 m		6 m	
Brain region	WT	R6/1	WT	R6/1	WT	R6/1
Striatum						
DA	9352 ± 1108	6414 ± 397*	6835 ± 2110	3674 ± 1057**	8491 ± 1446	1786 ± 207***
DOPAC	1644 ± 179	1059 ± 260*	1295 ± 135	732 ± 210**	1157 ± 164	458 ± 83***
HVA	780 ± 76	505 ± 47	629 ± 146	330 ± 81*	843 ± 28	366 ± 111***
DOPAC/DA	0.19 ± 0.03	0.17 ± 0.05	0.17 ± 0.03	0.21 ± 0.03	0.14 ± 0.02	0.26 ± 0.03**
5-HT	301 ± 21	272 ± 31	206 ± 36	267 ± 24	196 ± 53	218 ± 61
5-HIAA	231 ± 17	131 ± 14	167 ± 39	103 ± 15.8	186 ± 20	112 ± 25*
5-HIAA/5-HT	0.77 ± 0.02	0.51 ± 0.1*	0.79 ± 0.05	0.39 ± 0.07***	1.27 ± 0.37	0.56 ± 0.08
NA	77 ± 9.5	76.2 ± 17	66 ± 25.6	96.2 ± 11.5	69.8 ± 26	51 ± 12
Substantia nigra						
DA	294 ± 40	232 ± 26	412 ± 112	128 ± 33**	176 ± 18.6	84 ± 27.5*
DOPAC	166 ± 346	96 ± 146	192 ± 36	78 ± 18**	92 ± 10	48 ± 14.3**
HVA	192 ± 14.7	132 ± 18	247 ± 55	117 ± 19*	nd	nd
DOPAC/DA	0.59 ± 0.12	0.432 ± 0.08	0.59 ± 0.17	0.65 ± 0.08	0.52 ± 0.02	0.72 ± 0.24
5-HT	200 ± 37	163 ± 34	281 ± 54	146 ± 22	259 ± 62	186 ± 12.3
5-HIAA	128 ± 9.8	88 ± 11.8*	165 ± 36	78 ± 12.8*	240 ± 100	168 ± 47.2
5-HIAA/5-HT	0.78 ± 0.22	0.568 ± 0.05	0.59 ± 0.08	0.56 ± 0.08	0.84 ± 0.21	0.92 ± 0.28
NA	297 ± 50	220 ± 19.7	269 ± 51	160 ± 29	139 ± 29	86 ± 20
Globus pallidus						
DA	845 ± 353	530 ± 119	1378 ± 608	224 ± 53**	565 ± 206	113 ± 41**
DOPAC	251 ± 62	212 ± 37	395 ± 93	117 ± 38	164 ± 53	50 ± 12.6
DOPAC/DA	0.73 ± 0.31	0.438 ± 0.16	0.47 ± 0.17	0.77 ± 0.08	0.41 ± 0.07	0.66 ± 0.17
5-HT	175 ± 34	133 ± 8.1	346 ± 30	123 ± 40	221 ± 39	167 ± 25
5-HIAA	342 ± 50	229 ± 44	562 ± 99	392 ± 191	288 ± 56	161 ± 26
5-HIAA/5-HT	2.26 ± 0.59	1.76 ± 0.38	1.99 ± 0.4	2.91 ± 0.52	1.39 ± 0.26	1.06 ± 0.24
Motor cortex						
5-HT	165 ± 15.9	108 ± 40	117 ± 31	101 ± 12.6	247 ± 68	82 ± 17.5
5-HIAA	335 ± 61	241 ± 101	291 ± 81	325 ± 71	305 ± 61	130 ± 26
5-HIAA/5-HT	2.06 ± 0.33	2.6 ± 0.53	2.57 ± 0.31	3.07 ± 0.6	1.33 ± 0.17	1.93 ± 0.53
NA	225 ± 15.6	251 ± 97	229 ± 50	209 ± 24	232 ± 30	140 ± 15
Dorsal Hippocampus						
5-HT	72 ± 4	69 ± 13	75 ± 19	63 ± 9.8	129 ± 20	115 ± 22
5-HIAA	225 ± 18	157 ± 12.4	239 ± 51	163 ± 25	216 ± 23	156 ± 8.5
5-HIAA/5-HT	3.19 ± 0.44	2.45 ± 0.38	3.36 ± 0.25	2.72 ± 0.42	1.86 ± 0.47	1.68 ± 0.45
NA	235 ± 25	277 ± 27	221 ± 45	224 ± 21	187 ± 38	161 ± 38
Ventral Hippocampus						
5-HT	309 ± 85	197 ± 84	318 ± 126	256 ± 97	200 ± 39	102 ± 35
5-HIAA	239 ± 22	146 ± 14.8*	313 ± 72	194 ± 33*	275 ± 25	128 ± 27**
5-HIAA/5-HT	0.98 ± 0.28	1.06 ± 0.29	1.28 ± 0.40	1.18 ± 0.40	1.51 ± 0.21	1.72 ± 0.47
NA	266 ± 19.7	239 ± 46	267 ± 37	221 ± 25	191 ± 42	146 ± 28
Thalamus						
5-HT	150 ± 39	82 ± 6.8	85 ± 14.2	72 ± 8.2	122 ± 34	76 ± 20
5-HIAA	224 ± 23	143 ± 41	158 ± 9.7	110 ± 14	213 ± 32	144 ± 40
5-HIAA/5-HT	1.86 ± 0.47	1.92 ± 0.73	2.83 ± 0.59	1.72 ± 0.49	2.25 ± 0.71	3.57 ± 1.94
NA	173 ± 28	208 ± 26	160 ± 14.1	152 ± 16.4	160 ± 30	125 ± 10

Results are expressed as mean ± SEM values (pg/mg of tissue) in the striatum, substantia nigra, globus pallidus, motor cortex, dorsal and ventral hippocampus and the thalamus of wild type (WT) and R6/1 mice at 2, 4 and 6 months of age. Data are from 4 to 5 mice per group at each age, $*p < 0.05$, $**p < 0.01$ and $***p < 0.001$ (Student t-test). nd – not detected.

5-HT was lower as early as 2 months in the striatum of R6/1 mice (Table 1). The levels of NA were similar in R6/1 and WT mice in all brain regions whatever the age considered (Table 1).

3.1. DA, 5-HT, and NA neurochemical markers at PND35 in R6/1 and WT mice

The second series of experiment addressed the quantitative distribution and qualitative analysis of monoaminergic systems in the selected 18 brain regions in early stage of development (PND35). Table 2 reports the number of animals per genotype considered in the statistical treatment of the data for each brain region and parameter. The table also reports the mean weight of tissues. DA and HVA contents were significantly lower in the nAC of R6/1 mice as compared to WT mice. Conversely, DA and DOPAC contents in GP were significantly higher in R6/1 mice as compared to WT mice. The content of DA and its metabolites in other brain regions was not significantly different between R6/1 and WT mice (Table 3a). Similarly, the NA, 5-HT and its metabolite 5-HIAA content were not significantly different in all the brain regions between R6/1 mice and WT mice (Table 3b). The ratio DOPAC/DA and 5-HIAA/5-HT were similar in all brain regions between the two mouse genotypes (Tables 3a and 3b).

3.2. Qualitative analysis of the neurochemical indexes across the selected brain regions

The correlations between monoamines and their metabolites in the same brain regions are reported in Table 4 for WT and R6/1 mice. We found a strong correlation between DA and its metabolite DOPAC in the cortex (OFC, aMC and Th) and VTA of WT mice which was absent in R6/1 mice. In contrast, there was a strong correlation between DA and DOPAC in VLS and GP of R6/1 mice. A positive correlation was also seen between DA and DOPAC in SN of both the WT mice and R6/1 mice. A negative correlation between DA and DOPAC was reported in Am of R6/1 mice. We also found strong correlations between DA and HVA in the cortical and striatal region of WT mice and less in R6/1

Table 2
Experimental details. The table reports the name of the brain structures (and the corresponding abbreviation) that have been chosen for the second experiment, the mean size of punched brain region (in mg ± SEM) (see also Fig. 1), and the number of mice considered for the statistical analysis for each brain region. No significant differences were observed between the weight of tissue between WT and R6/1 mice (data not shown). Starting from 11 mice/group, lower numbers are due to accidental manipulations, loss of chromatographic signal (sometimes below detection limit (not dectected, nd), loss of tissue, and/or outliers. DA turnover (t), DOPAC/DA, 5-HT t, 5-HIAA/5-HT.

Brain regions	Abbr.	weight	values (n)/group (WT/R6/1)							
		(mg ± SEM)	DA	DOPAC	HVA	5-HT	5-HIAA	NA	DA t	5-HT t
Cortex										
orbitofrontal	OFC	1.73 ± 0.17	9/10	9/11	nd	9/11	8/11	9/10	10/9	9/11
prelimbic	PL	2.07 ± 0.15	8/11	8/11	9/11	7/11	9/11	7/11	8/11	7/11
infralimbic	IL	0.92 ± 0.14	9/10	10/11	10/11	10/11	10/11	10/10	8/9	11/10
Anterior motor cortex	aMC	2.55 ± 0.14	6/10	7/10	7/10	7/10	8/10	8/9	6/9	8/10
posterior motor cortex	pMC	2.97 ± 0.24	7/11	11/11	11/10	11/11	11/11	10/11	7/11	10/9
Nucleus accumbens Striatum										
Nucleus accumbens	nAC	1.87 ± 0.14	11/11	11/11	11/11	11/10	11/11	11/9	11/11	11/10
Dorsomedial striatum	DMS	1.01 ± 0.12	7/7	8/7	8/7	8/7	8/7	7/6	7/7	7/7
Ventromedial striatum	VMS	1.84 ± 0.11	11/11	11/11	11/11	11/11	11/11	10/9	11/11	11/11
Dorsolateral striatum	DLS	1.57 ± 0.12	11/10	11/10	11/11	11/11	11/11	7/6	11/10	11/11
Ventrolateral striatum	VLS	1.94 ± 0.08	11/11	11/11	11/11	11/11	11/11	9/9	11/11	11/11
Basal ganglia mesencephalon										
Globus pallidus	GP	1.51 ± 0.11	11/11	11/11	11/11	11/11	11/11	10/11	11/11	11/11
Substantia nigra	SN	1.76 ± 0.16	11/11	11/11	11/10	10/11	10/11	11/11	10/11	11/11
Ventral tegmental area	VTA	1.67 ± 0.15	10/11	10/11	10/11	10/11	10/10	10/11	10/11	10/11
Dorsal raphe nucleus	DRN	2 ± 0.14	10/10	10/10	9/10	10/9	10/10	10/10	10/9	10/10
Other regions										
Thalamus	Th	1.72 ± 0.12	9/9	9/10	10/10	11/10	10/11	11/10	9/9	10/10
Amygdala	Am	1.74 ± 0.13	10/10	11/10	11/9	8/10	10/10	9/8	10/9	8/10
Hippocampus Dorsal/anterior parts	dHP	2.35 ± 0.15	7/5	8/5	nd	11/11	10/11	11/11	6/5	10/11
Cerebellum	Cb	4.35 ± 0.37	9/11	10/10	9/8	10/11	11/11	11/11	10/11	11/11

mice. The correlations between DOPAC and HVA in cortical regions (IL and pMC), GP and VTA of R6/1 mice were absent in WT mice. Conversely, we observed strong correlations between DOPAC and HVA in Cb and striatal region of WT mice. Of note, we performed a similar analysis with NA considering that NA fibers could also be involved in the direct regulations of DA (precursor), DOPAC and HVA contents. Very few correlations were reported between the content of these molecules and NA content (data not shown). However, in the OFC and the Cb, NA content correlated with DOPAC and HVA contents in WT (data not shown).

The 5-HT and its metabolite 5-HIAA in WT and R6/1 mice were correlating in striatal regions, pMC and DRN only. The 5-HT and 5-HIAA content was correlating in the cortex (IL, aMC and Th), Cb, VTA and SN of R6/1 mice but not WT mice. Unexpectedly, negative correlations between 5-HT and 5-HIAA were reported in PL and Am of WT mice (Table 4).

We analysed the correlations of DA, 5-HT or the ratios DOPAC/DA and 5-HIAA/5-HT across the 18 selected brain regions in WT and R6/1 mice (Fig. 2). As expected in WT mice (Fitoussi et al., 2013), the number of significant correlations for DA tissue content was low,

Table 3a
Tissue content of dopamine and its metabolites in various brain regions of WT and R6/1 mice at PND35.

	DA		DOPAC		HVA		DOPAC/DA	
Brain region	WT	R6/1	WT	R6/1	WT	R6/1	WT	R6/1
OFC	10.9 ± 5.6	3.42 ± 0.76	35.2 ± 12.8	13.3 ± 1.6	76.2 ± 23	101 ± 18.9	5.69 ± 0.85	4.35 ± 0.57
PL	34.4 ± 3.6	29.5 ± 4.7	24.4 ± 5.1	22.6 ± 3.5	14.3 ± 2.3	14.7 ± 3.1	0.69 ± 0.12	1.01 ± 0.25
IL	85.6 ± 23.4	61.5 ± 7.5	48.5 ± 6.5	47 ± 12.6	35.7 ± 4.4	38.6 ± 7.1	0.53 ± 0.07	1.09 ± 0.31
aMC	21.6 ± 6.6	23.3 ± 8.7	59.5 ± 11.1	57.2 ± 10.8	14.9 ± 1.2	109 ± 1.9	3.19 ± 1.02	5.19 ± 1.66
pMC	15.6 ± 2.9	21.1 ± 1.9	26.3 ± 3.31	24.2 ± 3.4	29.5 ± 3.8	32.6 ± 2.8	1.14 ± 0.13	1.82 ± 0.35
Th	59.8 ± 25	25.8 ± 8.2	84.7 ± 3	42.3 ± 8.9	329 ± 58.7	465 ± 86.4	2.31 ± 0.45	2.26 ± 0.48
dHP	12.3 ± 4.1	5.68 ± 0.67	9.7 ± 2.7	5.26 ± 0.74	nd	nd	1.20 ± 0.22	0.75 ± 0.01
Am	176 ± 25.3	269 ± 33.7	118 ± 17.3	138 ± 24.8	59.7 ± 9.4	59.3 ± 7.5	0.67 ± 0.1	0.95 ± 0.12
Cb	5.36 ± 1.01	7.02 ± 1.08	13.6 ± 2.9	12.6 ± 1.1	89.9 ± 18.1	102 ± 22.9	2.25 ± 0.25	2.34 ± 0.29
nAC	3135 ± 329	2112 ± 225*	2365 ± 367	1810 ± 146	2474 ± 218	1860 ± 147*	0.88 ± 0.18	1.08 ± 0.17
VMS	2708 ± 364	2268 ± 306	1821 ± 216	2194 ± 368	1752 ± 155	1763 ± 214	0.83 ± 0.15	1.17 ± 0.24
DMS	3456 ± 252	2506 ± 382	1924 ± 487	1973 ± 326	2544 ± 366	2284 ± 325	0.66 ± 0.13	0.85 ± 0.17
VLS	3682 ± 475	3424 ± 422	1941 ± 273	1857 ± 214	3020 ± 336	2885 ± 338	0.55 ± 0.07	0.57 ± 0.03
DLS	4211 ± 537	4477 ± 536	2062 ± 254	2014 ± 173	3007 ± 269	2690 ± 289	0.52 ± 0.07	0.48 ± 0.05
GP	305 ± 50.4	521 ± 80.3*	250 ± 39.9	412 ± 57*	1150 ± 120	1498 ± 141	0.99 ± 0.14	0.82 ± 0.05
VTA	278 ± 32.9	323 ± 36	284 ± 22.2	387 ± 45.6	747 ± 86.3	924 ± 112	1.09 ± 0.08	1.10 ± 0.08
SN	154 ± 24.8	182 ± 18.9	128 ± 16.3	148 ± 16	486 ± 67.5	562 ± 46	0.83 ± 0.09	0.84 ± 0.07
DRN	116 ± 10.7	127 ± 22.5	42.2 ± 7.1	52.1 ± 8.4	53.3 ± 7.6	70 ± 16.9	0.39 ± 0.08	0.34 ± 0.03

Results are expressed as mean ± SEM values (pg/mg of tissue) in various brain regions of wild type (WT) and R6/1 mice, except for DOPAC/DA (ratio). Starting from 11 mice per group, the final number of observations/group is reported in Table 2 for each parameter and brain regions. *$p < 0.05$ (Student t-test). nd – not detected.

Table 3b
Tissue content of NA, 5-HT and its metabolite 5-HIAA in various brain regions of WT and R6/1 mice at PND35.

Brain region	NA		5-HT		5-HIAA		5-HIAA/5-HT	
	WT	R6/1	WT	R6/1	WT	R6/1	WT	R6/1
OFC	47.4 ± 9.7	39 ± 5.4	33.5 ± 8.4	26.7 ± 3.6	87.8 ± 19.3	126 ± 21.7	3.45 ± 0.71	5.31 ± 0.83
PL	77.6 ± 4.9	73.7 ± 10.8	173 ± 71.6	242 ± 83.8	110 ± 15.6	71.6 ± 14.4	4.09 ± 1.92	3.84 ± 1.64
IL	205 ± 35.8	171 ± 31.1	106 ± 20.8	119 ± 26	127 ± 24	148 ± 30.4	1.39 ± 0.14	1.79 ± 0.55
aMC	nd	nd	197 ± 16.6	147 ± 17.4	249 ± 51.3	117 ± 14.5	1.08 ± 0.14	0.85 ± 0.11
pMC	208 ± 14.9	222 ± 26.2	363 ± 50.4	288 ± 44.8	127 ± 24.5	109 ± 18	0.35 ± 0.04	0.35 ± 0.39
Th	181 ± 14.6	144 ± 20	205 ± 25.3	205 ± 23.7	380 ± 37.9	394 ± 54.1	2.21 ± 0.27	2.09 ± 0.23
dHP	65.3 ± 10.9	70.5 ± 5.2	88.4 ± 14.7	84.2 ± 5.2	395 ± 31.6	402 ± 55.5	5.20 ± 0.35	4.90 ± 0.74
Am	220 ± 24.4	121 ± 51.2	272 ± 75.3	252 ± 74.5	169 ± 26.8	232 ± 28.4	1.34 ± 0.46	2.4 ± 0.6
Cb	102 ± 18.1	81.2 ± 7.8	56 ± 11.5	62.9 ± 8.9	227 ± 41.2	236 ± 43	4.12 ± 0.66	3.8 ± 0.5
nAC	54.1 ± 14.3	53.2 ± 16.9	156 ± 21.9	104 ± 12.8	411 ± 37	346 ± 51	2.91 ± 0.26	3.16 ± 0.35
VMS	50.9 ± 10.4	79.2 ± 10.7	70.6 ± 10.4	76.3 ± 13.9	270 ± 24.3	301 ± 17.3	4.46 ± 0.54	5.55 ± 1.02
DMS	20.8 ± 5.1	21.1 ± 8.6	84 ± 11	81 ± 17.9	256 ± 50.2	212 ± 29.8	2.68 ± 0.13	2.91 ± 0.3
VLS	38.4 ± 9.5	33 ± 4.9	79.9 ± 10.6	79.9 ± 10.4	240 ± 31.4	214 ± 24.2	3.03 ± 0.09	2.78 ± 0.18
DLS	29.3 ± 4.7	20 ± 5.6	67.8 ± 8.4	69 ± 7.8	231 ± 24.9	197 ± 20.3	3.25 ± 0.2	3.01 ± 0.31
GP	71.8 ± 16.6	76.5 ± 19.9	128 ± 21.7	159 ± 18.5	277 ± 34.6	294 ± 27.3	2.39 ± 0.23	1.99 ± 0.18
VTA	100 ± 9.4	129 ± 12.4	162 ± 21	176 ± 21.4	366 ± 50.2	439 ± 53.3	2.35 ± 0.26	2.57 ± 0.25
SN	84.8 ± 14.2	87.6 ± 13.8	228 ± 35.1	387 ± 48.5	315 ± 44.1	461 ± 53.5	1.49 ± 0.21	1.28 ± 0.14
DRN	175 ± 18.1	213 ± 25.5	1077 ± 191	1431 ± 279	336 ± 76.5	516 ± 65.1	0.39 ± 0.07	0.41 ± 0.07

Results are expressed as mean ± SEM values (pg/mg of tissue) in various brain regions of wild type (WT) and R6/1 mice, except for 5-HIAA/5-HT (ratio). Starting from 11 mice per group, the final number of observations/group is reported in Table 2 for each parameter and brain regions. There were no significant differences between genotypes (Student t-test). nd – not detected.

reaching only 8 correlations. The number of significant correlations was similar in R6/1 but the pattern was totally different from WT with no correlation of DA tissue content between striatal and cortical regions. The number of correlations for 5-HT tissue content was slightly reduced in R6/1 mice (7 instead of 10 in WT). The correlations in WT and R6/1 mice were also different except for the pairs dHP/VMS and OFC/VTA. As also previously reported (Dellu-Hagedorn et al., 2017), the number of correlations of the DOPAC/DA ratio is slightly higher (13) in WT mice, compared to the neurotransmitter itself, with most correlations including striatal (including nAC) territories. Interestingly, some correlations were reported between the ratio DOPAC/DA in the regions containing DA cell bodies and striatum or between striatal quadrants. The number of correlations for DOPAC/DA was strongly decreased in R6/1 mice with no correlations reported between the different striatal quadrants or between VTA/SN and striatum (Fig. 2). A reduction of the number of correlations was also reported for 5-HIAA/5-HT in R6/1 mice (6 correlations) compared to WT (10 correlations) mice. Only the DRN/DMS correlation was reported for the two genotypes. NA tissue content in WT mice was also correlating in 8 cases including two negative ones (data not shown) and mostly involving striatal quadrants (7 out the 8). The number of correlations in R6/1 mice was reduced to only 4, all positive and 3 still engaging the striatal quadrants.

We then analyze possible correlations of the combination of 5-HT and DA contents or the DOPAC/DA and 5-HIAA/5-HT ratios across the brain regions (Fig. 3). In WT mice, neurotransmitters content correlated between the basal ganglia and other brains regions and also within the OFC. Also 6 out of 18 5-HT/DA correlations were found in the same brain regions. In R6/1 mice, the number of correlations was slightly reduced (18 instead of 23 in WT) with a higher proportion of negative correlations and lesser number of correlations found in the same brain regions. There was a higher proportion of cortico-cortical/thalamic correlations. The 5-HT/DA correlation in the VLS was the only one

Table 4
Correlative analysis for the tissue content of DA and 5-HT with their respective metabolites within the same brain region of WT and R6/1 mice at PND35.

	DA vs DOPAC		DA vs HVA		DOPAC vs HVA		5-HT vs 5-HIAA	
Brain region	WT	R6/1	WT	R6/1	WT	R6/1	WT	R6/1
OFC	$p < 0.001$	NS	$p < 0.05$	NS	$p < 0.01$	NS	NS	NS
PL	NS	NS	NS	$p < 0.05$	NS	NS	*$p < 0.01$*	NS
IL	NS	NS	NS	NS	NS	$p < 0.01$	NS	$p < 0.01$
aMC	$p < 0.05$	NS	$p < 0.05$	NS	NS	NS	NS	$p < 0.05$
pMC	NS	NS	NS	NS	NS	$p < 0.001$	$p < 0.001$	$p < 0.01$
Th	$p < 0.01$	NS	NS	NS	NS	NS	NS	$p < 0.05$
dHP	NS	NS	NS	NS	NS	NS	NS	NS
Am	NS	*$p < 0.05$*	NS	NS	NS	NS	*$p < 0.05$*	NS
Cb	NS	NS	NS	NS	$p < 0.01$	NS	NS	$p < 0.05$
nAC	NS	NS	NS	NS	$p < 0.05$	$p < 0.05$	NS	NS
VMS	NS	NS	$p < 0.05$	NS	NS	NS	NS	NS
DMS	NS	NS	NS	$p < 0.01$	$p < 0.01$	NS	$p < 0.05$	$p < 0.05$
VLS	NS	$p < 0.001$	$p < 0.001$	$p < 0.001$	$p < 0.01$	$p < 0.001$	$p < 0.001$	$p < 0.001$
DLS	NS	NS	$p < 0.001$	NS	$p < 0.01$	NS	NS	NS
GP	NS	$p < 0.001$	$p < 0.05$	$p < 0.01$	NS	$p < 0.05$	$p < 0.001$	$p < 0.05$
VTA	$p < 0.01$	NS	$p < 0.05$	NS	NS	$p < 0.001$	NS	$p < 0.05$
SN	$p < 0.05$	$p < 0.05$	NS	$p < 0.001$	$p < 0.01$	$p < 0.05$	NS	$p < 0.05$
DRN	NS	NS	NS	NS	NS	NS	$p < 0.01$	$p < 0.05$

Correlations (linear regression, Pearson's r) between the parent neurotransmitter and its metabolite(s) in same brain regions. The content (pg/mg) of DA and its metabolites, 5-HT and its metabolite did correlate in some cases. All significant correlations were positive except three (shown in italic). The number of values for each genotype depends on each parameter and brain regions as reported in Table 2. NS, not significant.

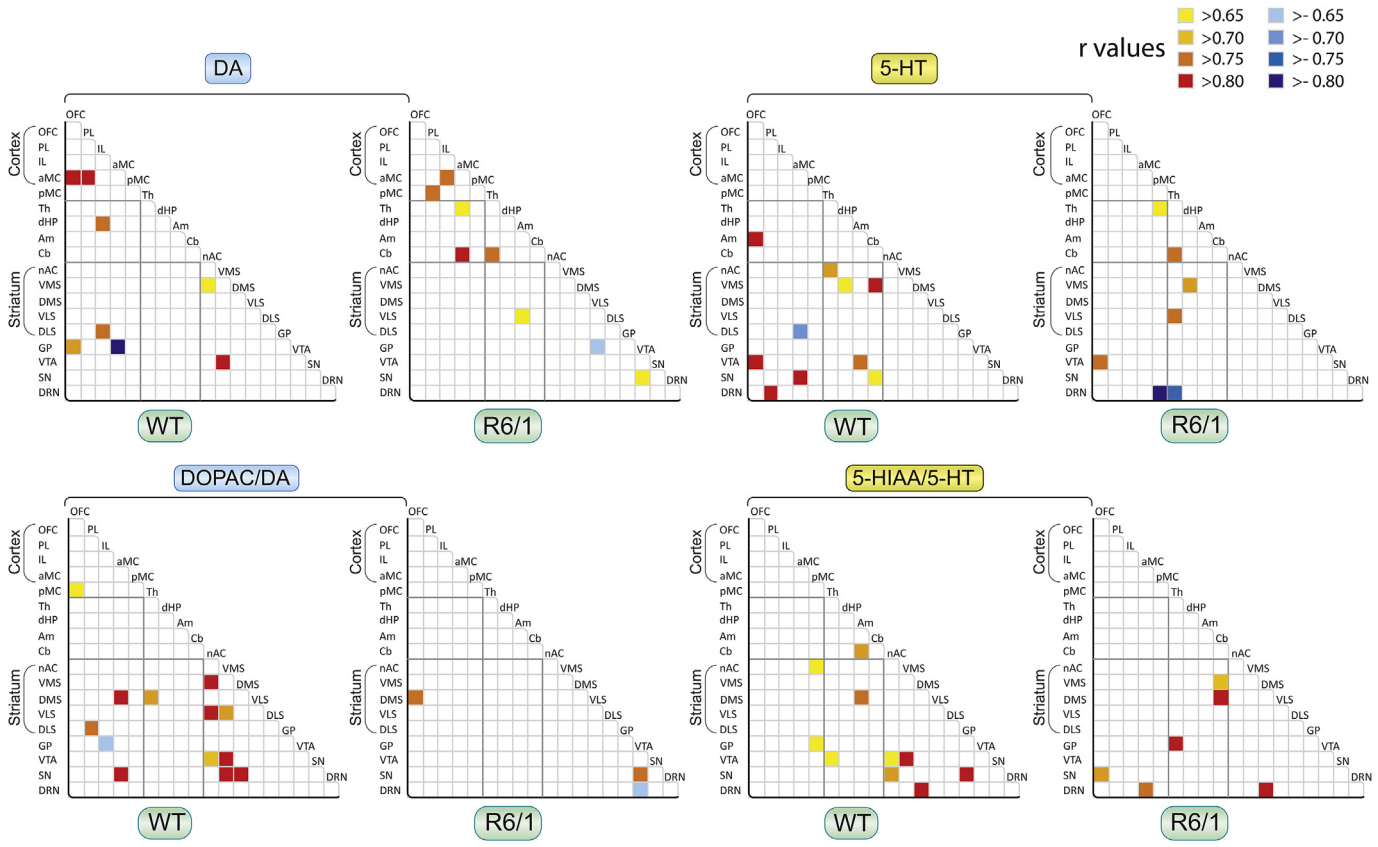

Fig. 2. Qualitative analysis of the neurochemical indexes of monoamines across the selected brain regions. Representation of the range of Pearson's r values for each linear regression, of DA, 5-HT tissue contents (pg/mg) and the ratio DOPAC/DA and 5-HIAA/5-HT between the 18 brain areas of R6/1 mice and wild type mice at PND35 age. Colored boxes correspond to the existence of a significant correlation between the two parameters (yellow to red: positive; blue: negative) considered after correction for multiple comparisons. The number of values for each linear regression is reported in Table 2.

present in both genotypes.

We found stronger correlation between DA and 5-HT in same striatal region of WT mice as compared to R6/1 mice, whereas there are few positive correlations in the same cortical region of two strains of mice but more negative correlation is observed in R6/1 mice (Fig. 3). Twenty nine correlations between DOPAC/DA and 5-HIAA/5-HT were reported in WT, including 4 within the same brain region. The correlations are marked by the ability of DA rich areas (striatum, VTA, SN) to correlate with the 5-HT turnover index of different regions. The number of correlations was reduced in R6/1 to 18 with a loss of striato/striatal and striato/mesencephalic correlations. However, the correlations increased within the brain regions themselves. In both genotypes, the correlations were mostly positive.

We also looked at the correlations established between NA and DA tissue content and NA and 5-HT tissue content across selected brain regions (data not shown). In R6/1 mice, the number of NA/DA correlations was slightly higher (19 instead of 14 in WT) with a higher proportion of negative correlations (8 instead 3 in WT) and lesser number of correlations found in the same brain regions (2 instead of 3 in WT). Conversely, the number of NA/5-HT correlations was slightly diminished (16 instead of 21 in WT) with a lesser proportion of negative correlations (5 instead 3 in WT) and substantially lesser number of correlations found in the same brain regions (1 instead of 5 in WT). For both DA/NA and 5-HT/NA analyses, the correlations involving the OFC (4 or 5 respectively) were reduced to only one. There were more correlations involving IL, PL and/or VMS for NA/DA. WT correlations in VTA or Am (5 or 4 each) for 5-HT/NA were reduced in R6/1 mice.

4. Discussion

We report in the R6/1 mice a progressive failure of the dopaminergic pathways linking the mesencephalon to the striatum/nAC and the relative protection of the ascending 5-HT/NA neuronal systems. Qualitative modifications of monoamines distribution were detected very early in striatal quadrants and beyond. The modified pattern of monoamines in young R6/1 mice would parallel early disturbances of neurobiological networks involved in affective, cognitive and motor functions.

One important finding is the temporal and progressive decrease of all dopaminergic compounds at 2, 4 and 6 months in R6/1 mice, reaching 80% decrease for tissue DA at 6 months. Two previous studies did not report a significant decrease in striatal DA, DOPAC and HVA contents at 15–16 weeks old R6/1 mice (Petersen et al., 2002; Pineda et al., 2005), even though a decreased extracellular DA concentration was reported (Petersen et al., 2002). Conversely, our data agree with the reduction of DA tissue content in both male and female R6/1 mice at 8 weeks (Renoir et al., 2014). Furthermore, we report that DA tissue levels were reduced in the SN and the GP with a delayed temporality compared to the striatum. Consistently, it has been reported in the YAC128 and R6/2 models of HD reduced levels of DA tissue content (Callahan and Abercrombie, 2011; Garcia-Miralles et al., 2016; Reynolds et al., 1999) and DA release (Callahan and Abercrombie, 2011; Hickey et al., 2002; Kaplan et al., 2018).

The whole temporal study from PND35 to 6 months is disparate (two distinct experiments with different ways of punching) with noticeable differences of quantities in the striatum of youngest WT mice. It could be explained by technical issues, the pieces collected for the second experiment being smaller and more fragile (Dellu-Hagedorn

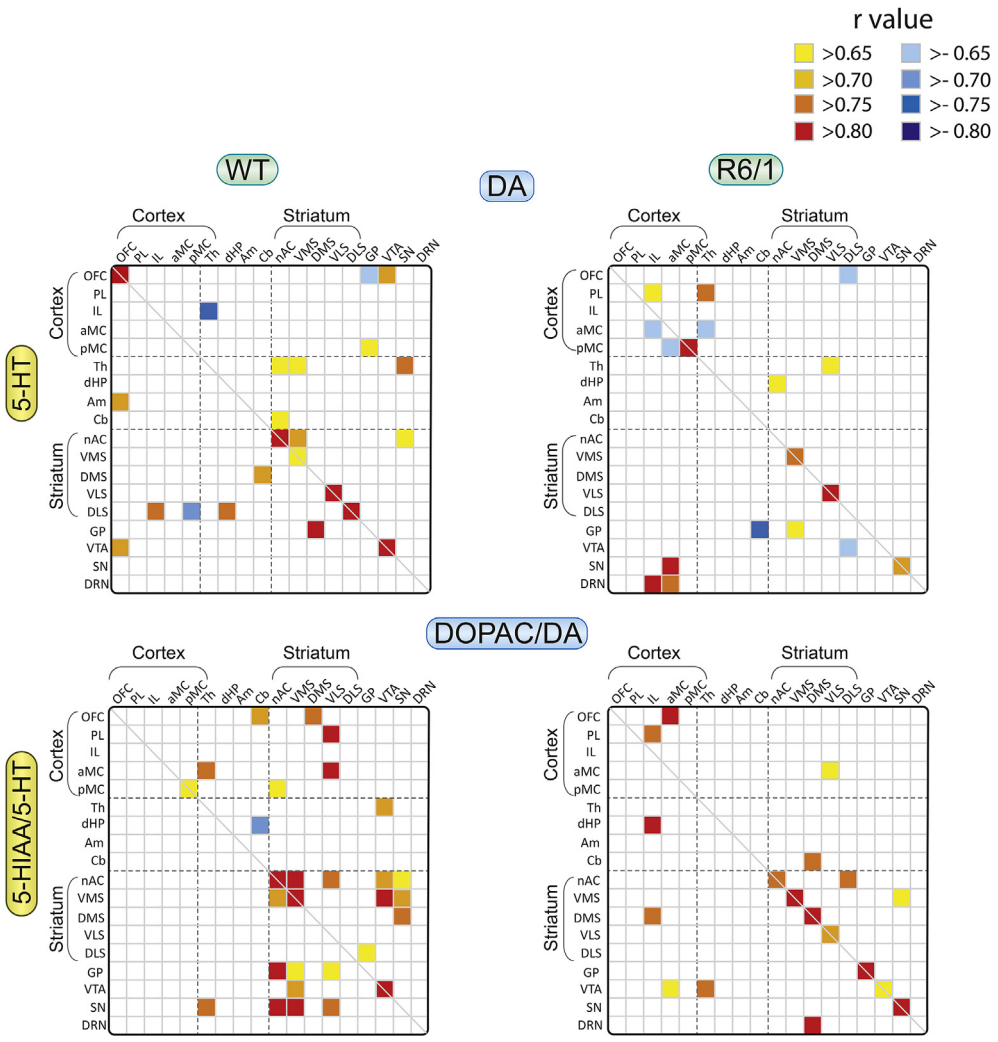

Fig. 3. Correlative analysis between the monoamine content across the brain areas. Representation of the range of Pearson's r values for each linear regression between 5-HT and DA contents (first row) and between 5-HT/5-HIAA and DOPAC/DA contents (second row) within and between the 18 brain areas of R6/1 mice and wild type mice at PND35 age. Colored boxes correspond to the existence of a significant correlation between the two parameters (yellow to red: positive; blue: negative) considered after correction for multiple comparisons. The number of values each linear regression is reported in Table 2.

et al., 2017). Additionally, the quantities of DA increase between 1 and 4 months ((Mochel et al., 2011), unpublished observations). Thus, considering the whole temporal study, our data extent the proposal that DA neurons are impaired in an age-dependent manner in R6/1 (Ortiz et al., 2011) and R6/2 mice (Mochel et al., 2011).

The reduction of DA would be compatible with a loss of innervation combined with metabolic issues rather than the degeneration of DA neurons. Indeed, the number of tyrosine hydroxylase labelled neurons in the SN was found to be similar at 16 weeks in WT and R6/1 mice (Petersen et al., 2002). A loss of innervation is possible because the DA cell bodies in the SN were reported to be smaller (Petersen et al., 2002), associated with a decrease in autoradiographic labelling and function of the DA transporter in the striatum of R6/1 (Ortiz et al., 2011) and R6/2 (Kaplan et al., 2018) mice, respectively. Moreover, the increase in the DOPAC/DA ratio in the striatum of R6/1 mice at 6-months is due to the higher loss of DA compared to DOPAC (or HVA). This result is compatible with a possible lower ability of DA neurons to maintain DA in storage vesicles as suggested in R6/2 mice (Johnson et al., 2007; Ortiz et al., 2010).

Early alteration could start in the mesoaccumbens DA pathway in R6/1 mice and not in the different quadrants of the striatum in which no transient increase in striatal DA levels could be observed (Chen et al., 2013; Jahanshahi et al., 2010). Although the ventral parts of the striatum have been reported to be relatively spared compared to dorsal parts in R6/2 mice (Kaplan et al., 2018), decreased DA levels have been observed in the nAC of HD patients (Bedard et al., 2011). DA release in the nAC has been shown to be reduced in the Q175 knock-in HD mouse model associated with reduced motivational behaviour (Covey et al., 2016). Paradoxically, we report an increase in DA tissue content in the GP at this early stage. We have no explanation to account for this result. Speculatively, it could correspond to DA fibres that normally reach the nAC and the striatum which stopped their progression in the GP, leading to this transient and early increase.

Our correlative analyses suggest that central DA transmission is profoundly altered at PND35. As we presently report in WT mice, the ratio DOPAC/DA more than the DA content correlates between striatal quadrants as well as with other brain regions in Wistar rats (Dellu-Hagedorn et al., 2017; Fitoussi et al., 2013). This pattern, which could be a functional counterpart of the ascending spiral linking the nAC to the DLS (Haber et al., 2000) is totally disrupted in R6/1 mice. The striatal dynamic imposed by DA neurotransmission is altered at PND35 suggesting that the proposed defect in DA connectivity (Chen et al., 2013) occurs very early. A role of the already decreased nAC DA levels in this pattern cannot be excluded.

The fate of 5-HT and NA neurons is dissimilar to DA ones. No tissue modification is found between R6/1 and their WT littermates whatever

the brain regions. Previous studies have reported an early increase followed by late decrease in brain NA content whereas 5-HT content was progressively decreased in R6/2 mice (Mochel et al., 2011; Reynolds et al., 1999). On the other hand, the lack of significant decrease in striatal 5-HT content is consistent with studies performed in R6/1 mice (Renoir et al., 2011) or YAC128 mice (Garcia-Miralles et al., 2016). While the variability we had cautions our interpretation, we found decreased levels of 5-HIAA in the SN, hippocampus and cortex at two months in line with a previous study (Renoir et al., 2011). Our data agree with the fact that the metabolite is much more affected than 5-HT itself in all the above cited studies, not only in the striatum. Such a decrease could be related to a diminished activity and/or expression of tryptophan hydroxylase (Yohrling et al., 2002; Renoir et al., 2011). Thus, as others, we could not confirm the increase in both striatal 5-HT tissue content and 5-HT fibres in HD mutation carriers compared to age-matched controls (Bedard et al., 2011; Kish et al., 1987). On the other hand, we highlight an early change of pattern of correlations of DA and 5-HT turnovers, centred in mesencephalon/striatum in WT toward local correlations in single brain regions in R6/1 mice, notably the striatum.

The poor number of correlations between a compound and its metabolite in a single brain region contrasts with our previous study in Wistar rats in keeping in mind that the age of the animals (6 months) and their number (35) were different (Dellu-Hagedorn et al., 2017). It suggests that the tissue parameters come from heterogeneous, metabolic links within a single tissue, at least in young tissues. The pattern was changing between WT and R6/1 notably for 5-HT with a higher proportion of correlations in R6/1 mice. For DA metabolism, the NA system is a possible source of heterogeneity because DA is produced by NA neurons with possible, visible consequences on metabolism and release of DA in the hippocampus and the cortex (Devoto et al., 2005; Kempadoo et al., 2016). However, we could observe very few correlations of NA versus DA, DOPAC or HVA which could be consistent with multiple origins of these compounds.

The overall set of neurochemical data allows us to comment on the early development of the disease. The accumulation of huntingtin has been reported at 1-month in R6/1 mice (Milnerwood et al., 2006). Early neurobiological impairments in R6/1 mice have been underscored from 2 to 4 months on LTP in the hippocampus (Milnerwood et al., 2006), GABAergic transmission in the GP (Du et al., 2016, 2017bib_Du_et_al_2016bib_Du_et_al_2017), procedural memory and local field potentials along the cortico-striatal pathway (Cayzac et al., 2011), affective and cognitive behaviours (Renoir et al., 2011, 2014), and altered behavioural responses to D1 receptor agonist (Renoir et al., 2014), largely before the onset of motor symptoms observed at 4 months (Menalled and Chesselet, 2002). Modification of brain functional connectivity has been reported at two months in R6/1 mice (Cabanas et al., 2017). Early affective-like disturbances are reported in other HD mouse models including BAC (Hult Lundh et al., 2013), YAC128 (Pouladi et al., 2009) or Hdh Q111 mice (Orvoen et al., 2012). Taken together, these data suggest that the maturation of numerous neurobiological networks is different in these mice models compared to their WT counterparts (Barnat et al., 2017), having for consequence the widespread impact we report on monoaminergic system organization across the brain at PND35. GABAergic neurons play an important integration role in coordinating neuronal activity in the brain including monoaminergic neuron regulation (Farrant and Nusser, 2005). Our findings suggest that altered connectivity in HD brain may arise from an early altered regulation of neuronal activity orchestrated by the diverse populations of GABAergic and monoaminergic neurons (Barry et al., 2018; Cepeda et al., 2013; Du et al., 2016).

In our R6/1 HD model, the progression of the disease leads to a profile resembling to the pathophysiology of Parkinson's disease for DA tissue content as suggested in humans (Bedard et al., 2011). The anti-parkinsonian drug L-DOPA could eventually ameliorate symptoms in R6/2 mice after short term treatment (Hickey et al., 2002) but the dose was 100 times higher than a normal regimen (De Deurwaerdere et al., 2017). The relative efficacy of tetrabenazine (Mestre et al., 2009), a blocker of the vesicular transporter type 2, seems paradoxical in view of the dopaminergic tone loss in HD. On the other hand, it could limit the monoamines imbalance accompanying the disease. DA and 5-HT transmissions could be targeted in the prodromal neuropsychiatric symptoms including apathy and behavioural disturbances. Additional data are warranted to further this possibility.

In conclusion, we provide evidence that monoamines are quantitatively and/or qualitatively altered at PND35 and we extent the proposal that DA neurons are progressively altered in the R6/1 model of HD. The early loss of DA connectivity across the brain could confer a higher sensitivity to a possible excitotoxic influence of corticostriatal and thalamostriatal glutamatergic transmission (Cepeda et al., 2014).

Acknowledgments

This work was supported by grants from Centre National de la Recherche Scientifique. Marion Garnerot and Laura Cardoit are acknowledged for technical supports.

References

Barnat, M., Le Friec, J., Benstaali, C., Humbert, S., 2017. Huntingtin-mediated multipolar-bipolar transition of newborn cortical neurons is critical for their postnatal neuronal morphology. Neuron 93, 99–114.
Barry, J., Akopian, G., Cepeda, C., Levine, M.S., 2018. Striatal direct and indirect pathway output structures are differentially altered in mouse models of huntington's disease. J. Neurosci. 38, 4678–4694.
Bedard, C., Wallman, M.J., Pourcher, E., Gould, P.V., Parent, A., Parent, M., 2011. Serotonin and dopamine striatal innervation in Parkinson's disease and Huntington's chorea. Park. Relat. Disord. 17, 593–598.
Benjamini, Y., Hochberg, Y., 1995. Controlling the False Discovery Rate: a practical and powerful approach to multiple testing. J. R. Stat. Soc. Ser. B 57, 289–300.
Cabanas, M., Bassil, F., Mons, N., Garret, M., Cho, Y.H., 2017. Changes in striatal activity and functional connectivity in a mouse model of Huntington's disease. PLoS One 12, e0184580.
Callahan, J.W., Abercrombie, E.D., 2011. In vivo dopamine efflux is decreased in striatum of both fragment (R6/2) and full-length (YAC128) transgenic mouse models of huntington's disease. Front. Syst. Neurosci. 5, 61.
Cayzac, S., Delcasso, S., Paz, V., Jeantet, Y., Cho, Y.H., 2011. Changes in striatal procedural memory coding correlate with learning deficits in a mouse model of Huntington disease. Proc. Natl. Acad. Sci. U. S. A. 108, 9280–9285.
Cepeda, C., Galvan, L., Holley, S.M., Rao, S.P., Andre, V.M., Botelho, E.P., Chen, J.Y., Watson, J.B., Deisseroth, K., Levine, M.S., 2013. Multiple sources of striatal inhibition are differentially affected in Huntington's disease mouse models. J. Neurosci. 33, 7393–7406.
Cepeda, C., Murphy, K.P., Parent, M., Levine, M.S., 2014. The role of dopamine in Huntington's disease. Prog. Brain Res. 211, 235–254.
Chagraoui, A., Whitestone, S., Baassiri, L., Manem, J., Di Giovanni, G., De Deurwaerdere, P., 2019. Neurochemical impact of the 5-HT2C receptor agonist WAY-163909 on monoamine tissue content in the rat brain. Neurochem. Int. 124, 245–255.
Chen, J.Y., Wang, E.A., Cepeda, C., Levine, M.S., 2013. Dopamine imbalance in Huntington's disease: a mechanism for the lack of behavioral flexibility. Front. Neurosci. 7, 114.
Covey, D.P., Dantrassy, H.M., Zlebnik, N.E., Gildish, I., Cheer, J.F., 2016. Compromised dopaminergic encoding of reward accompanying suppressed willingness to overcome high effort costs is a prominent prodromal characteristic of the Q175 mouse model of huntington's disease. J. Neurosci. 36, 4993–5002.
Dalley, J.W., Everitt, B.J., Robbins, T.W., 2011. Impulsivity, compulsivity, and top-down cognitive control. Neuron 69, 680–694.
De Deurwaerdere, P., Di Giovanni, G., 2017. Serotonergic modulation of the activity of mesencephalic dopaminergic systems: therapeutic implications. Prog. Neurobiol. 151, 175–236.
De Deurwaerdere, P., Di Giovanni, G., Millan, M.J., 2017. Expanding the repertoire of L-DOPA's actions: a comprehensive review of its functional neurochemistry. Prog. Neurobiol. 151, 57–100.
Dellu-Hagedorn, F., Fitoussi, A., De Deurwaerdere, P., 2017. Correlative analysis of dopaminergic and serotonergic metabolism across the brain to study monoaminergic function and interaction. J. Neurosci. Methods 15 (280), 54–63.
Dellu-Hagedorn, F., Rivalan, M., Fitoussi, A., De Deurwaerdere, P., 2018. Inter-individual differences in the impulsive/compulsive dimension: deciphering related dopaminergic and serotonergic metabolisms at rest. Philos. Trans. R. Soc. Lond. B Biol. Sci. 373.
Devoto, P., Flore, G., Saba, P., Fa, M., Gessa, G.L., 2005. Co-release of noradrenaline and dopamine in the cerebral cortex elicited by single train and repeated train stimulation of the locus coeruleus. BMC Neurosci. 6, 31.
Du, Z., Chazalon, M., Bestaven, E., Leste-Lasserre, T., Baufreton, J., Cazalets, J.R., Cho, Y.H., Garret, M., 2016. Early GABAergic transmission defects in the external globus pallidus and rest/activity rhythm alteration in a mouse model of Huntington's

disease. Neuroscience 329, 363–379.
Du, Z., Tertrais, M., Courtand, G., Leste-Lasserre, T., Cardoit, L., Masmejean, F., Halgand, C., Cho, Y.H., Garret, M., 2017. Differential alteration in expression of striatal GABAAR subunits in mouse models of huntington's disease. Front. Mol. Neurosci. 10, 198.
Farrant, M., Nusser, Z., 2005. Variations on an inhibitory theme: phasic and tonic activation of GABA(A) receptors. Nat. Rev. Neurosci. 6, 215–229.
Fitoussi, A., Dellu-Hagedorn, F., De Deurwaerdere, P., 2013. Monoamines tissue content analysis reveals restricted and site-specific correlations in brain regions involved in cognition. Neuroscience 255, 233–245.
Franklin, K.B.J., Paxinos, G., 2007. The mouse brain in stereotaxic coordinates. In: Press, A. (Ed.), third ed. Elsevier, New York, pp. 256.
Garcia-Miralles, M., Ooi, J., Ferrari Bardile, C., Tan, L.J., George, M., Drum, C.L., Lin, R.Y., Hayden, M.R., Pouladi, M.A., 2016. Treatment with the MAO-A inhibitor clorgyline elevates monoamine neurotransmitter levels and improves affective phenotypes in a mouse model of Huntington disease. Exp. Neurol. 278, 4–10.
Haber, S.N., Fudge, J.L., McFarland, N.R., 2000. Striatonigrostriatal pathways in primates form an ascending spiral from the shell to the dorsolateral striatum. J. Neurosci. 20, 2369–2382.
Hickey, M.A., Reynolds, G.P., Morton, A.J., 2002. The role of dopamine in motor symptoms in the R6/2 transgenic mouse model of Huntington's disease. J. Neurochem. 81, 46–59.
Hult Lundh, S., Nilsson, N., Soylu, R., Kirik, D., Petersen, A., 2013. Hypothalamic expression of mutant huntingtin contributes to the development of depressive-like behavior in the BAC transgenic mouse model of Huntington's disease. Hum. Mol. Genet. 22, 3485–3497.
Jahanshahi, A., Vlamings, R., Kaya, A.H., Lim, L.W., Janssen, M.L., Tan, S., Visser-Vandewalle, V., Steinbusch, H.W., Temel, Y., 2010. Hyperdopaminergic status in experimental Huntington disease. J. Neuropathol. Exp. Neurol. 69, 910–917.
Johnson, M.A., Villanueva, M., Haynes, C.L., Seipel, A.T., Buhler, L.A., Wightman, R.M., 2007. Catecholamine exocytosis is diminished in R6/2 Huntington's disease model mice. J. Neurochem. 103, 2102–2110.
Kaplan, S.V., Limbocker, R.A., Levant, B., Johnson, M.A., 2018. Regional differences in dopamine release in the R6/2 mouse caudate putamen. Electroanalysis 30, 1066–1072.
Kempadoo, K.A., Mosharov, E.V., Choi, S.J., Sulzer, D., Kandel, E.R., 2016. Dopamine release from the locus coeruleus to the dorsal hippocampus promotes spatial learning and memory. Proc. Natl. Acad. Sci. U. S. A. 113, 14835–14840.
Kish, S.J., Shannak, K., Hornykiewicz, O., 1987. Elevated serotonin and reduced dopamine in subregionally divided Huntington's disease striatum. Ann. Neurol. 22, 386–389.
Klouche, M.S., De Deurwaerdere, P., Dellu-Hagedorn, F., Lakhdar-Ghazal, N., Benomar, S., 2015. Monoamine content during the reproductive cycle of Perna perna depends on site of origin on the Atlantic Coast of Morocco. Sci. Rep. 5, 13715.
Martinez-Horta, S., Perez-Perez, J., van Duijn, E., Fernandez-Bobadilla, R., Carceller, M., Pagonabarraga, J., Pascual-Sedano, B., Campolongo, A., Ruiz-Idiago, J., Sampedro, F., Landwehrmeyer, G.B., Kulisevsky, J., 2016. Neuropsychiatric symptoms are very common in premanifest and early stage Huntington's Disease. Park. Relat. Disord. 25, 58–64.
Menalled, L.B., Chesselet, M.F., 2002. Mouse models of Huntington's disease. Trends Pharmacol. Sci. 23, 32–39.
Mestre, T., Ferreira, J., Coelho, M.M., Rosa, M., Sampaio, C., 2009. Therapeutic interventions for symptomatic treatment in Huntington's disease. Cochrane Database Syst. Rev., Cd006456.
Milnerwood, A.J., Cummings, D.M., Dallerac, G.M., Brown, J.Y., Vatsavayai, S.C., Hirst, M.C., Rezaie, P., Murphy, K.P., 2006. Early development of aberrant synaptic plasticity in a mouse model of Huntington's disease. Hum. Mol. Genet. 15, 1690–1703.
Mochel, F., Durant, B., Durr, A., Schiffmann, R., 2011. Altered dopamine and serotonin metabolism in motorically asymptomatic R6/2 mice. PLoS One 6, e18336.
Ortiz, A.N., Kurth, B.J., Osterhaus, G.L., Johnson, M.A., 2010. Dysregulation of intracellular dopamine stores revealed in the R6/2 mouse striatum. J. Neurochem. 112, 755–761.
Ortiz, A.N., Kurth, B.J., Osterhaus, G.L., Johnson, M.A., 2011. Impaired dopamine release and uptake in R6/1 Huntington's disease model mice. Neurosci. Lett. 492, 11–14.
Orvoen, S., Pla, P., Gardier, A.M., Saudou, F., David, D.J., 2012. Huntington's disease knock-in male mice show specific anxiety-like behaviour and altered neuronal maturation. Neurosci. Lett. 507, 127–132.
Petersen, A., Puschban, Z., Lotharius, J., NicNiocaill, B., Wiekop, P., O'Connor, W.T., Brundin, P., 2002. Evidence for dysfunction of the nigrostriatal pathway in the R6/1 line of transgenic Huntington's disease mice. Neurobiol. Dis. 11, 134–146.
Pineda, J.R., Canals, J.M., Bosch, M., Adell, A., Mengod, G., Artigas, F., Ernfors, P., Alberch, J., 2005. Brain-derived neurotrophic factor modulates dopaminergic deficits in a transgenic mouse model of Huntington's disease. J. Neurochem. 93, 1057–1068.
Pittaras, E., Callebert, J., Chennaoui, M., Rabat, A., Granon, S., 2016. Individual behavioral and neurochemical markers of unadapted decision-making processes in healthy inbred mice. Brain Struct. Funct. 221, 4615–4629.
Pouladi, M.A., Graham, R.K., Karasinska, J.M., Xie, Y., Santos, R.D., Petersen, A., Hayden, M.R., 2009. Prevention of depressive behaviour in the YAC128 mouse model of Huntington disease by mutation at residue 586 of huntingtin. Brain 132, 919–932.
Ramos, A.R.S., Garrett, C., 2017. Huntington's disease: premotor phase. Neurodegener. Dis. 17, 313–322.
Renoir, T., Argyropoulos, A., Chevarin, C., Lanfumey, L., Hannan, A.J., 2014. Sexually dimorphic dopaminergic dysfunction in a transgenic mouse model of Huntington's disease. Pharmacol. Biochem. Behav. 127, 15–20.
Renoir, T., Zajac, M.S., Du, X., Pang, T.Y., Leang, L., Chevarin, C., Lanfumey, L., Hannan, A.J., 2011. Sexually dimorphic serotonergic dysfunction in a mouse model of Huntington's disease and depression. PLoS One 6, e22133.
Reynolds, G.P., Dalton, C.F., Tillery, C.L., Mangiarini, L., Davies, S.W., Bates, G.P., 1999. Brain neurotransmitter deficits in mice transgenic for the Huntington's disease mutation. J. Neurochem. 72, 1773–1776.
Simic, G., Babic Leko, M., Wray, S., Harrington, C.R., Delalle, I., Jovanov-Milosevic, N., Bazadona, D., Buee, L., de Silva, R., Di Giovanni, G., Wischik, C.M., Hof, P.R., 2017. Monoaminergic neuropathology in Alzheimer's disease. Prog. Neurobiol.
Yohrling, I.G., Jiang, G.C., DeJohn, M.M., Robertson, D.J., Vrana, K.E., Cha, J.H., 2002. Inhibition of tryptophan hydroxylase activity and decreased 5-HT1A receptor binding in a mouse model of Huntington's disease. J. Neurochem. 82, 1416–1423.